Tellus SERIES B CHEMICAL AND PHYSICAL METEOROLOGY
PUBLISHED BY THE INTERNATIONAL METEOROLOGICAL INSTITUTE IN STOCKHOLM

Tellus (2010), 62B, 1–13
Printed in Singapore. All rights reserved

© 2009 The Authors
Journal compilation © 2010 Blackwell Munksgaard
TELLUS

A recent build-up of atmospheric CO_2 over Europe. Part 1: observed signals and possible explanations

By MICHEL RAMONET[1,*], PHILIPPE CIAIS[1], TUULA AALTO[4], CÉLINE AULAGNIER[1], FRÉDÉRIC CHEVALLIER[1], DOMENICO CIPRIANO[5], THOMAS J. CONWAY[6], LASZLO HASZPRA[2], VICTOR KAZAN[1], FRANK MEINHARDT[3], JEAN-DANIEL PARIS[1], MARTINA SCHMIDT[1], PETER SIMMONDS[7], IRÈNE XUEREF-RÉMY[1] and JAROSLAW N. NECKI[8] [1]*Laboratoire des Sciences du Climat et de l'Environnement (LSCE/IPSL), CEA-CNRS-UVSQ, 91191 Gif sur Yvette, France;* [2]*Hungarian Meteorological Service, H-1675 Budapest, P.O. Box 39, Hungary;* [3]*Umweltbundesamt, Postfach 1229, 79196 Kirchzarten, Germany;* [4]*Finnish Meteorological Institute, Air Quality Research, Sahaajankatu 20E, 00880 Helsinki, Finland;* [5]*Centro Elettrotecnico Sperimentale Italiano, Via Rubattino 54–20134 Milano, Italy;* [6]*National Oceanic and Atmospheric Administration, Earth System Research Laboratory, 325 Broadway, Boulder, CO 80305, USA;* [7]*School of Chemistry, University of Bristol, Bristol, UK;* [8]*AGH University of Science and Technology, Krakow, Poland*

(Manuscript received 11 March 2009; in final form 2 September 2009)

ABSTRACT

We analysed interannual and decadal changes in the atmospheric CO_2 concentration gradient (ΔCO_2) between Europe and the Atlantic Ocean over the period 1995–2007. Fourteen measurement stations are used, with Mace-Head being used to define background conditions. The variability of ΔCO_2 reflects fossil fuel emissions and natural sinks activity over Europe, as well as atmospheric transport variability. The mean ΔCO_2 increased by 1–2 ppm at Eastern European stations (~30% growth), between 1990–1995 and 2000–2005. This built up of CO_2 over the continent is predominantly a winter signal. If the observed increase of ΔCO_2 is explained by changes in ecosystem fluxes, a loss of about 0.46 Pg C per year would be required during 2000–2005. Even if severe droughts have impacted Western Europe in 2003 and 2005, a sustained CO_2 loss of that magnitude is unlikely to be true. We sought alternative explanations for the observed CO_2 build-up into transport changes and into regional redistribution of fossil fuel CO_2 emissions. Boundary layer heights becoming shallower can only explain 32% of the variance of the signal. Regional changes of emissions may explain up to 27% of the build-up. More insights are given in the Aulagnier et al. companion paper.

1. Introduction

The European continent is a major source of CO_2 to the atmosphere. This source is caused by fossil fuel CO_2 emissions, but ameliorated by terrestrial ecosystem uptake (NEE). Over geographic Europe, emissions from fossil fuel combustion and cement production amount to 1.82 ± 0.18 PgC yr^{-1} during the 1990s (Marland et al., 2007). Terrestrial uptake, mostly located in forests and grasslands, is estimated to be 0.11 ± 0.28 PgC yr^{-1} over the same time period (Janssens et al., 2003). This gives a net CO_2 flux of 1.71 ± 0.33 PgC yr^{-1}. The relative error of the European sink is larger than the one of fossil CO_2 emissions, and hence dominates the uncertainty of the net CO_2 flux. At the regional and local scale, however, the uncertainty of fossil CO_2 emissions increases when country emission statistics get disaggregated in space and time using uncertain activity maps and emission factors (P. Ciais, personal communication, 2009), and may dominate over the uncertainty of NEE. The goal of this study is to assess a recent build-up of CO_2 over the European continent, deduced from long-term continuous timeseries of atmospheric CO_2 concentration measurements. The atmosphere is a fast, but incomplete mixer of the surface fluxes. Therefore, time and space gradients in atmospheric CO_2 concentration over Europe must reflect either changes in net CO_2 flux, or changes in atmospheric transport, or a combination of both. Obtaining estimates of the net CO_2 flux from concentration measurements requires solving the inverse problem of inverting the atmospheric transport (Gurney et al., 2002; Rödenbeck et al., 2003), or to use another tracer with a known emission field analogous to CO_2, such as for instance Rn-222, to infer unknown CO_2 fluxes

*Corresponding author.
e-mail: michel.ramonet@lsce.ipsl.fr
DOI: 10.1111/j.1600-0889.2009.00442.x

(Schmidt et al., 1996; Levin et al., 1999; Biraud et al., 2000; Schmidt et al., 2003). Here, we do not wish to determine the net CO_2 flux of Europe, but rather to assess the *trend* in that flux that would be needed to explain the observed build-up of CO_2. Alternatively, we also examine how trends in boundary layer height could have explained the build-up signal by a simple dilution effect.

What do we know about trends in CO_2 emissions and sinks over Europe? At first glance, the fossil CO_2 emissions (UNFCCC, 2006; Marland et al., 2007) are quite stable, with only a small increase of 0.27% yr^{-1} during the period 1995–2007 for EU-27. In fact, fossil CO_2 emissions first decreased from 1995 to 2000 (-0.50% yr^{-1}), and then re-increased from 2000 to 2006 (0.70% yr^{-1}). To analyse trends in NEE, we have ecosystem model simulations (Vetter et al., 2007) and forest biomass inventories data (Nabuurs et al., 2002). Forest biomass inventories have a typical revisit time of 5 yr or so, and can only be used for long-term trend detection. These data suggest a slight reduction in the forest biomass C sink between the 1980s and the 1990s (Nabuurs et al., 2002) at a rate of 0.017 PgC yr^{-2} over EU15 countries excluding Luxembourg but including Switzerland and Norway. Simulations from ecosystem models (Vetter et al., 2007) indicate that the NEE is a sink, which has slightly increased between 1990 and today. These models only account for climate and rising CO_2 drivers, but ignore forest aging and management effects. Hence, they cannot be seen as realistic tools to explore trends in NEE.

A difficulty hindering detection of decadal trends of CO_2 fluxes is the strong interannual variability. Year-to-year changes are small for fossil CO_2 emissions, but large for NEE (Bousquet et al., 2000). This is because NEE responds strongly to climate variability, as a result of climate-sensitive photosynthesis and respiration fluxes. Ecosystem models and atmospheric inversions results agree on the amplitude of interannual NEE fluctuations, found to be on the order of 0.3 PgC yr^{-1} at continental level over Europe (Peylin et al., 2005; Baker et al., 2006; Vetter et al., 2007). Oppositely, these two approaches do not agree for the phase of NEE anomalies, except maybe for particularly large events, such as the CO_2 abnormal loss caused by extreme drought and heat during the summer 2003 (Ciais et al., 2005; Reichstein et al., 2005).

What do we know about decadal trends in atmospheric transport affecting CO_2 gradients among stations? At stations distributed globally (GLOBALVIEW-CO_2, 2006), we know that interannual variation in transport has a smaller impact than variation in fluxes in contributing to interannual CO_2 gradients (Bousquet et al., 2000; Rödenbeck et al., 2003; Baker et al., 2006). Whether decadal trends in transport have or not a smaller impact than decadal trends in fluxes in explaining trends in CO_2 gradients remains an unresolved question. In this study, we address this question by analysing the evolution in the CO_2 accumulation over Western Europe over the period 1990–2007. First, we quantify the variability of CO_2 from a European atmospheric network of 14 stations (Sections 2 and 3), and the trends in the CO_2 gradient (ΔCO_2) between the continent and the Atlantic Ocean (Section 4). We then analyse the build-up of CO_2 detected in winter between 2000–2005 and 1995–2000, and two of its possible causes: changes in vertical mixing due to boundary layer heights becoming more shallow (Section 5), and changes in the regional distribution of fossil CO_2 emissions (Section 6).

2. Atmospheric CO_2 variability from European stations

2.1. *Station network and sampling frequency*

The CO_2 variability over the past 14 yr is analysed from a data set of 14 long-term measurement stations of the CARBOEUROPE-IP and NOAA-GMD monitoring programmes. These stations are shown in Fig. 1 and their main characteristics summarized in Table 1. There are four marine stations: Izana (IZO), Mace-Head data (MHD), Iceland (ICE) and Station M (STM). There are four continental low-altitude stations, Baltic Sea (BAL), Black Sea Coast (BSC), Hegyhátsál (HH1) and to some extent Pallas (PAL) a 600 m high smooth hill. There are four mountain-top stations, Puy de Dome (PUY), Plateau Rosa (PRS), Schauinsland (SCH) and Kasprowy (KAS). The last site is Orleans (ORL), an aircraft site where vertical profiles are collected regularly between 100 and 3000 m above the ground. More detailed information about each station can be found in the Supporting Information.

The period of analysis extends from 1995 to 2007, but the records of MHD, SCH, HH1 and BAL are longer. We focus on the trend and interannual variability of the CO_2 gradient (ΔCO_2) between stations in the interior of the continent and the marine stations over the Atlantic. The Atlantic stations define the reference used to calculate ΔCO_2. The time step of trend analysis is monthly. CO_2 is measured weekly at flask sampling sites, and monthly/bi-weekly at the ORL aircraft site. CO_2 is measured each hour at the other in situ stations. At continental stations, atmospheric transport, local vegetation fluxes and emissions create significant variability of CO_2 on hourly to daily timescales (Gerbig et al., 2006). It is hence safer for analysing trends in ΔCO_2, to select data from continuous records in order to minimize this local noise.

2.2. *Stations calibration*

The CO_2 measurements analysed here are contributed by seven laboratories (Table 1). Each laboratory reports CO_2 in the WMO-93 or WMO-XX scale using national standards calibrated by NOAA/GMD. Each lab also participates to several intercomparison programs. Four WMO round robins (RR) intercomparison exercises (Pearman, 1993) organized by NOAA/GMD between 1991 and 2004 show an agreement better than 0.3 ppm between NOAA/GMD and LSCE, UBA, CESI laboratories [http://gaw.kishou.go.jp/wcc/co2/co2comparison.html]. For the

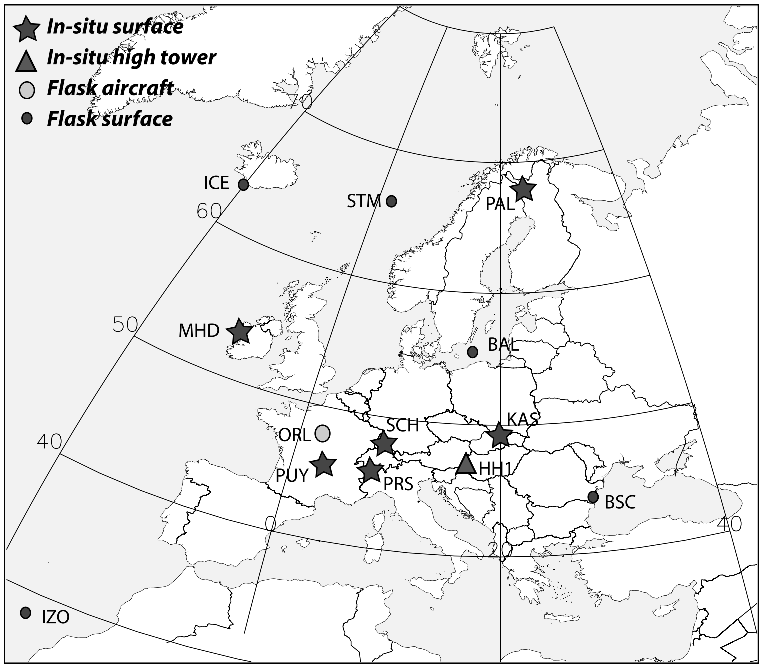

Fig. 1. Map of the monitoring sites including surface in situ (stars), high towers (triangle), aircraft grab sampling (big circle) and surface grab sampling sites (black circles).

Table 1. List of monitoring sites

Station	ID	Country	Latitude	Longitude	Alt (in a.s.l.)	Institute	Measurement
Mace Head	MHD	Ireland	53.3°	−9.9°	15	LSCE	In situ and flask
Iceland	ICE	Iceland	63.3°	−20.3°	118	ESRL	Flask
Station M	STM	Norway	66 0°	2.0°	0	ESRL	Flask
Izana	IZO	Spain	28.3°	−16.5°	2360	ESRL	Flask
Plateau Rosa	PRS	Italy	46 9°	7.7°	3480	CESİ	In situ
Schauinsland	SCH	Germany	47.9°	7.9°	1205	ÜBA	In situ
Pallas	PAL	Finland	68 0°	24.1°	560	FMİ	In situ
Orleans	ORL	France	47.8°	2.5°	250–3000	LSCE	Flask
Puy de Dome	PUY	France	45 8°	3.0°	1465	LSCE	In situ
Kasprowy	KAS	Poland	49,2°	20.0°	1989	AGH	In situ
Hegylıâtsâl	HH1	Hungary	47.0°	16.7°	248	HMS	In situ
Baltic Sea	BAL	Poland	55 4°	17.2°	3	ESRL	Flask
Black Sea Coast	BSC	Romania	44.2°	28.7°	3	ESRL	Flask

Note: Absolute values and linear slopes (=trends) of ΔCO_2 calculated for the continental sites over different periods and seasons.

Hungarian station, the earlier RR results showed large discrepancies but the measurement was done at this time at the K-puszta station with an outdated system. The data from this station are not used in this study. In addition to these RR, which take place only every 4 yr, we also compared CO_2 in weekly MHD flasks analysed by NOAA/GMD with the in situ record of LSCE. For the period 1995–2008, the mean difference between flask and in situ CO_2 is -0.08 ± 0.4 ppm. Similar results have been obtained within the Sausage Flask Intercomparison of the CARBOEUROPE-IP program [http://ce-atmosphere.lsce.ipsl.fr/]. In the Sausage Intercomparison, a difference of -0.03 ± 0.1 ppm between LSCE and NOAA/GMD is obtained, based upon 30 set of flasks filled with the same air. In summary, changes in ΔCO_2 due to interlaboratories calibration differences are unlikely to exceed 0.2 ppm. A bias between pairs of laboratories is quite unlikely to be synchronous, and hence unlikely to explain the observed coherent increase in ΔCO_2 with time (see Section 3).

2.3. *Data selection*

We assume that the variability of CO_2 on daily times scales, related to synoptic transport acting on regional sources, has not changed during the period of analysis. This variability is assumed to be noise superimposed on slower seasonal and interannual variations. The raw hourly CO_2 data from each in situ station (HH1, SCH, KAS, PUY, PRS and MHD) are fitted with a four-harmonics curve and a second order polynomial, and the residuals from this fit filtered in the time domain using a low-pass filter (Thoning et al., 1989). Time-domain filtering retains only CO_2 concentration variations on time scales greater than approximatively 80 d. Smoothed monthly CO_2 values were then determined from the smoothed curves formed by adding the polynomial with the harmonics and the filtered residuals.

For each in situ station, a data selection scheme has been defined to minimize effects of local contributions, and increase the representativeness of each record (see the Supporting Information). Data selection consists of retaining mid-afternoon data at the mountaintop station PAL and at the tall tower HH1, and of retaining nighttime data under windy conditions at the mountaintop station SCH. We will test the sensitivity of the ΔCO_2 increasing trend to this assumed data selection, in Section 4.

2.4. *Monthly CO_2 gradients between Europe and Atlantic ocean*

Monthly smoothed CO_2 curves are shown in Fig. 2. We observe that the CO_2 seasonal cycle amplitude increases between the Western European stations (MHD, ORL, PUY, PRS and SCH) and the Central/Eastern European stations (KAS, HH1, BAL and BSC). The mid-afternoon seasonal cycle amplitude is largest at the HH1 tall tower, where the influence of regional NEE is strong. The seasonal cycle amplitude attenuates at mountain-top sites, where boundary layer air influenced by regional fluxes is mixed with free tropospheric air influenced by more remote fluxes.

The choice of a marine reference is of key importance to estimate the CO_2 accumulation over Europe, ΔCO_2. All the marine stations show less variability than the continental ones, thus defining a marine reference CO_2 curve. We chose the MHD selected for marine baseline conditions as the reference for calculating ΔCO_2. MHD has a continuous record, thus well suited to establish a marine reference. It is also well positioned in latitude to define the marine background for most continental stations (Fig. 1). The current MHD marine selection established by Bousquet et al. (1997) and called MHD_{rbc} retains only hourly values influenced by North Atlantic air masses, based on local wind direction and speed and on hourly CO_2 variability criteria. We calculate ΔCO_2 at each station by determining the difference to the MHD_{rbc} curve. We will test in Section 4 some alternative marine reference stations, the NOAA/ESRL MHD flask record, STM, IZO or ICE.

Figure 3 provides the seasonal evolution of ΔCO_2 for three typical continental stations, Baltic Sea (BAL), Black Sea Coast (BSC) and Hegyhátsál (HH1). In winter, the three stations all show positive ΔCO_2 values, implied by soil respiration and fossil fuel emissions. The mean winter ΔCO_2 gradient is higher at HH1 (12.1 ppm) than at BAL (8.4 ppm). In winter, advection transports CO_2 from the continent to the ocean, and vertical

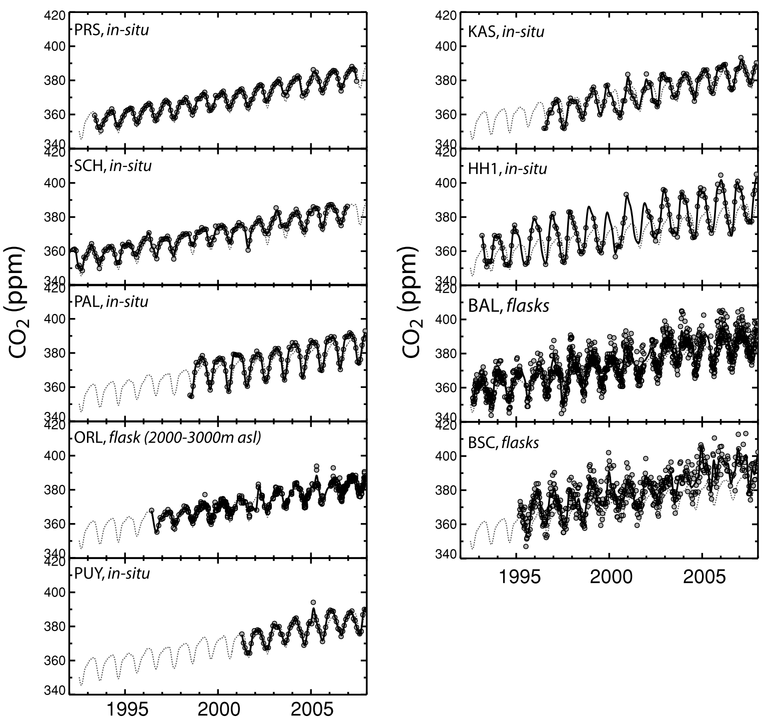

Fig. 2. Long-term atmospheric CO_2 records for the European carbon balance, during the past 14 yr (1992–2007). Hourly in situ records are been filtered in the time domain to remove variations on time scales shorter than approximatively 2 months. For in situ stations each dot represents monthly mean, whereas for flask sampling sites it represents a single air sample. The dotted grey line shows the fitting curves obtained from the in situ monitoring at Mace Head.

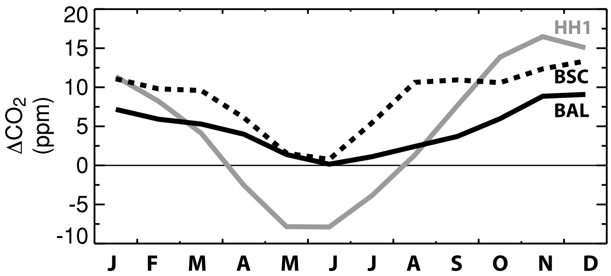

Fig. 3. Mean monthly CO_2 gradients between the coastal site of Mace Head and the continental sites of Hegyhátsál (grey), Baltic (black) and Black Sea Coast (dashed line).

mixing is reduced, producing high ΔCO_2 values. In summer, CO_2 at continental stations hardly drops below the marine background, and ΔCO_2 take small negative values. The first reason for this is that the NEE sink of CO_2 barely offsets fossil emissions (Vetter et al., 2007). Secondly, vertical mixing is more vigorous in summer, diluting the net CO_2 flux into convective boundary layers, typically 1000–1500 m thick. This increased vertical mixing contributes to make the negative summertime ΔCO_2 gradient much smaller in absolute value than the wintertime positive ΔCO_2 gradient.

3. Build-up of CO_2 and what it implies for trends in fluxes

Figure 4 shows the mean annual ΔCO_2 at each station. The smallest ΔCO_2 of -0.15 ± 0.6 ppm is found at the mountain-top station PRS which lies in the free-troposphere (Table 2). The largest ΔCO_2 of 8.6 ± 2.5 ppm is found at the low altitude station BSC, near the coast of the Black Sea, a station possibly affected by respired CO_2 displaced over the sea by nighttime drainage winds (Perez-Landa et al., 2007). The key result of this study is that, during the six consecutive years of 2000–2005, a persistent upward trend of ΔCO_2 is observed at seven stations out of nine in total. In contrast, ΔCO_2 is seen to be very stable over the preceding period 1995–2000. For instance between 1995–2000 and 2000–2005, ΔCO_2 increased linearly from 1.42 to 1.65 ppm at SCH (+16%) and from 3.6 to 4.6 ppm at HH1 (+28%).

The annual CO_2 build-up is predominantly a winter signal (Table 2). Fig. 5 compares the linear trend of ΔCO_2 in winter (DJF) and in summer (JJA) over three periods: 1990/1995, 2000/2005 and 2001/2006. The early 2000s periods are the ones for which ΔCO_2 is found to increase linearly at most stations. 2001–2006 is also the period chosen by Aulagnier et al. (2009) for analysis with the CHIMERE transport model. The stations with the largest DJF positive trend are BSC, HH1 and BAL. In early 2000s, low-altitude stations HH1, BSC and BAL show a greater trend on average ($\sim$0.75 ppm yr^{-1}) than mountain-top stations SCH, PUY, PRS and the ORL aircraft ($\sim$0.50 ppm yr^{-1}).

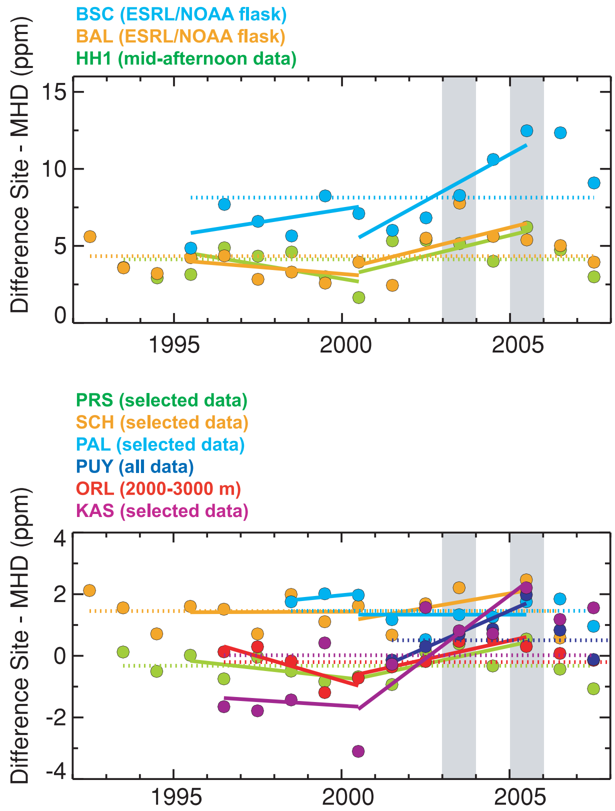

Fig. 4. Recent trends in the CO_2 difference between continental sites (data selection in text) and the reference curve of Mace Head in the marine sector. Each dot is the yearly mean CO_2 value at each site compared to Mace Head. The coloured dotted lines represent the long-term mean CO_2 difference during the full period years. The grey vertical bands mark years 2003 and 2005, during which extensive drought prevailed in temperate and central Europe and in southwestern Europe, respectively.

For JJA, during the 2001–2006 period, a decreasing trend of ΔCO_2 is found instead. The stations with the largest JJA negative trend of ΔCO_2 are HH1, BAL and SCH. For all the stations, the persistent build-up of 2000–2005 is followed in 2006 or in 2007 by a return to the 1995–2000 low ΔCO_2 value; representating interannual to decadal variability.

Applying a linear trend analysis to seasonal ΔCO_2 values rather than to annual values (Table 2) reveals that the 2000–2005 build-up is essentially a winter /spring phenomenon, and that there is no significant ΔCO_2 trend in European ΔCO_2 in summer (see the Supporting Information). But one can observe in Fig. 4 that ΔCO_2 was maximum in summer 2003 and 2005. Summer 2003 being marked by drought and heat, and 2005 by winter and spring drought in Southwestern Europe (Fink et al., 2004; Vautard et al., 2005). These dryer and warmer years could have simultaneously reduced the NEE sink and increased the boundary layer thickness by augmenting sensible heat emission.

Table 2. Absolute values and linear slopes (=trends) of ΔCO_2 calculated for the continental sites over different periods and seasons

Station	ID	ΔCO2 1995–2000 ppm	ΔCO2 2000–2005 ppm	Annual 1995–2000 (ppm/yr)	Annual 2000–2005 (ppm/yr)	Annual 1995–2007 (ppm/yr)	Winter 1995–2000 (ppm/yr)	Winter 2000–2005 (ppm/yr)	Winter 1995–2007 (ppm/yr)	Summer 1995–2000 (ppm/yr)	Summer 2000–2005 (ppm/yr)	Summer 1995–2007 (ppm/yr)	Spring 1995–2000 (ppm/yr)	Spring 2000–2005 (ppm/yr)	Spring 1995–2007 (ppm/yr)	Autumn 1995–2000 (ppm/yr)	Autumn 2000–2005 (ppm/yr)	Autumn 1995–2007 (ppm/yr)
Plateau Rosa	PRS	−0.46 ± 0.4	−0.15 ± 0.6	−0.12	0.23	0.01	−0.19	0.53	0.06	−0.08	−0.02	−0.17	−0.20	0.25	0.04	−0.01	0.18	0.06
Schauinsland	SCH	1.42 ± 0.4	1.65 ± 0.6	0.00	0.19	0.01	−0.17	0.43	0.13	0.32	−0.15	−0.07	−0.07	0.17	−0.05	−0.08	0.30	0.05
Pallas	PAL	1.91 ± 0.1	1.34 ± 0.5	−0.16	0.00	−0.05	0.52	0.17	0.12	0.26	−0.04	0.01	0.58	0.01	0.13	0.67	−0.14	0.05
Orléans	ORL	−0.33 ± 0.6	0.01 ± 0.5	−0.32	0.24	0.04	−0.02	0.49	0.09	−0.65	−0.15	−0.08	−0.49	0.64	0.15	0.17	−0.02	0.09
Puy de Dôme	PUY	–	0.74 ± 0.8	–	0.48	–	–	0.64	–	–	0.09	–	–	0.80	–	–	0.32	–
Kasprowy	KAS	−1.51 ± 1.3	0.32 ± 1.9	−0.07	0.82	0.36	0.61	0.28	0.40	0.32	0.61	0.41	−1.59	1.48	0.51	0.39	0.90	0.35
Hegyhátsál	HH1	3.60 ± 1.2	4.62 ± 1.6	−0.37	0.53	0.07	−0.66	0.75	0.11	0.54	−0.40	0.05	−1.17	1.04	0.03	−0.18	0.75	0.15
Baltic Sea	BAL	3.56 ± 0.8	5.11 ± 1.8	−0.19	0.54	0.23	−0.08	0.76	0.12	−0.34	0.50	0.32	−0.58	0.97	0.23	0.24	−0.08	0.25
Black Sea Coast	BSC	6.69 ± 1.3	8.55 ± 2.5	0.34	1.20	0.56	0.03	0.64	0.16	1.15	1.72	0.98	−0.09	1.01	0.42	−0.34	1.46	0.54

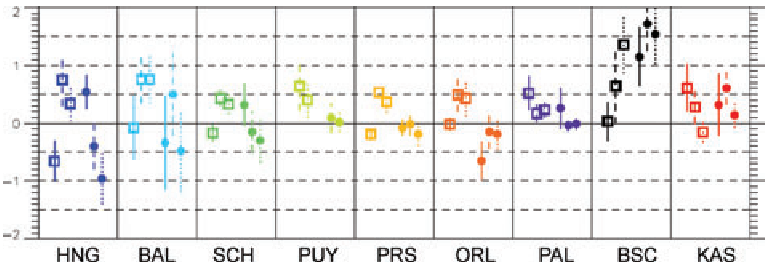

Fig. 5. Slopes of the linear fit (in ppm yr^{-1}) through seasonal mean CO_2 gradients in winter (squares) and summer (circles). For each season, the results are shown for three periods: 1995 to 2000 (left), 2000 to 2005 (middle) and 2001 to 2006 (right).

Scaling our best estimate of the European net CO_2 flux of 1.71 PgC yr^{-1} (see Section 1) by the ΔCO_2 ratio of 2000–2005 to 1995–2000, we deduce the existence of an extra source of CO_2 to the atmosphere amounting to 0.46 PgC yr^{-1} during the period 2000–2005. This extra CO_2 source amounts to a 27% higher net CO_2 flux each year. It is virtually impossible that increasing fossil CO_2 emissions alone can be the only driver of this extra CO_2 source. According to Marland et al. (2007) fossil CO_2 emissions in EU-27 have only increased by about 0.05 PgC (a growth of 0.3% yr^{-1}) between the mid 1990s and the early 2000s. By comparing several data set (UNFCCC, EDGARv3.2, CDIAC and GAINS), uncertainty of fossil fuel emissions inventories is estimated to 7% at the level of EU-27 (P. Ciais, personal communication). Assuming that atmospheric transport trends played no role in the ΔCO_2 trend, we can then deduce that terrestrial ecosystems have persistently lost more CO_2 during 2000–2005 than during 1995–2000. This would require updating the European terrestrial carbon sink of 0.11 $\pm$ 0.2 PgC yr^{-1} reported by Janssens et al. (2003) for 1990–1999 to a current source of 0.35 $\pm$ 0.2 PgC yr^{-1} for 2000–2005. Such a shift in NEE from sink to source await further analysis. In the next section, we analyse different sources of bias affecting this provocative conclusion. In Part 2 of this paper Aulagnier et al. (2009) use a mesoscale atmospheric transport model to further separate the contribution of NEE versus transport changes on the observed recent increase of ΔCO_2.

4. Sensitivity of the trend in ΔCO_2 to various settings

4.1. *Marine background CO_2 curve*

We tested the sensitivity of the trend in ΔCO_2 to the arbitrary choice of a marine reference station. The results are shown in the Supporting Information. At MHD, we tested three different marine reference curves constructed by using either (1) the NOAA/GMD weekly flasks sampled when the wind comes from a marine sector (see www.esrl.noaa.gov/gmd/ccgg/flask.html) or (2) the LSCE in situ CO_2 continuous record selected for marine conditions (Schmidt et al., 1996; Levin et al., 1999; Biraud et al., 2000; Schmidt et al., 2003) using local wind speed and direction criteria, or 3) the same record selected with wind modelled by the ECMWF Numerical Weather Prediction model over the grid point containing MHD. We also tested the impact of choosing for a marine reference the IZO continuous station, located on top of a 2360 m high mountain in the Canarias Is. (Navascues and Rus, 1991), or two other NOAA/GMD flask stations STM and ICE (Fig. 1).

The slope s of the linear trend of ΔCO_2 with time (year) over 2000–2005 is insensitive to the choice of a particular MHD reference curve (see the Supporting Information). Using the IZO instead of MHD as a reference station has the effect to increase s by the same constant value at each station ($+0.33 \pm 0.1$ ppm yr^{-1}) during 2000–2005 as compared 1995–2000. Using IZO as a reference does not change the relative differences in ΔCO_2 trend among the continental stations. Using IZO as a reference finally does not change our key result of a change from a zero or slightly negative ΔCO_2 during 1995–2000 to a positive ΔCO_2 during 2000–2005.

In additional sensitivity tests we calculated ΔCO_2 trends using as reference the NOAA/GMD flask stations of ICE and STM. Despite the fact that the absolute value of ΔCO_2 is sensitive to the choice of a marine reference, the ΔCO_2 trends between 2000–2005 and 1995–2000 is insensitive to that choice. Using ICE and STM as a reference gives a smaller slope s over 2000–2005 than when using MHD_{rbc} as reference. This is likely because the CO_2 values recorded at ICE and STM are influenced in winter by polluted air masses from Europe, as indicated by their high CO values (Szopa et al., 2007). Therefore, the two North Atlantic stations ICE and STM do not define as clean a marine background curve as the selected hourly MHD_{rbc}. To filter out the European influence from the ICE and STM records, one could remove CO_2 flasks data associated with elevated CO (e.g. deviating more than 2σ from the monthly CO curve).

4.2. *Selection of continuous data*

We have also investigated if the ΔCO_2 trends are robust to contrasted data selection at continuous stations. Because atmospheric mixing varies greatly during the day and between days, with NEE being coupled to these variations (Yi et al., 2004; Chen et al., 2005), data-selection methods have been developed and applied by experimentalists to filter out local influence at continentally influenced stations (Ramonet and Monfray, 1996; Brunke et al., 2004). In the Supporting

Information, we show the impact of different data-selection on the ΔCO_2 trend for continental stations SCH and HH1.

At SCH, a mid-elevation mountain top station reached during the summer days by nearby urban regional emissions in southern Germany, the current 'regional background' selection retains only windy night conditions (Schmidt et al., 2003). The ΔCO_2 increase between 1995–2000 and 2000–2005 is higher by 0.3 ppm yr^{-1} when full-time selection is applied instead of nighttime only (22:00–06:00 h).

At HH1, a tall tower station in a rural plain, CO_2 is minimum in the middle of the day in summer, with stable values being reached in the afternoon (12:00–16:00 h) when convection is established in the boundary layer. From comparison with a second site in the same area, mid-day selected CO_2 data at HH1 have been shown by (Haszpra, 1999) to be representative of an area of at least 100 km around the station. On the other hand, the nighttime CO_2 influenced by local respiratory sources, was shown to differ more greatly between the two towers. The ΔCO_2 increase between 1995–2000 and 2000–2005 is larger by 0.2 ppm yr^{-1} when mid-day (12–16 h) selection is applied. However, even if full-time data selection is considered, one would still observe a significant increase in ΔCO_2.

4.3. *Selection of flask data*

The BSC and BAL flask stations have the strongest increase in ΔCO_2 over the period 2000–2005 as compared to 1995–2000 (Fig. 4). Over water bodies surrounded by vegetated areas, advection of nighttime respired CO_2 by drainage winds, and recirculation by sea breezes creates complex mesoscale transport cells which impact the diurnal cycle of CO_2 (Nicholls et al., 2004; Perez-Landa et al., 2007). To minimize the sampling bias, a daytime sampling strategy is implemented at BSC and BAL by NOAA/GMD. However, the effects of re-circulated nighttime respired CO_2 may still be important in the day. If the flask-sampling hour of the day changes with time over several years, a temporal bias will be introduced in the CO_2 record. We hence analysed the trend in flask sampling hours at BSC and BAL between 1995 and 2005 (see the Supporting Information).

At BSC, the median of the sampling hour distribution each year has recently moved earlier by 50 min in 2004 and 2005 (7:22 UTC) as compared to 1995–2003 (8:10 UTC). At BAL, the flask sampling hour distribution is bimodal, with the nighttime and daytime ship passages, but there is no trend in sampling hour between 1994 and 2005. As a sensitivity test, we calculated the trend in ΔCO_2 that would be produced by selecting BSC flasks only between 0600 and 0900 UTC, and BAL flasks between 0800 and 1600 UTC (i.e. excluding nighttime). The resulting trends in ΔCO_2 are shown in the Supporting Information. There is almost no change in the ΔCO_2 increase between 1995–2000 and 2000–2005 at BSC, and an even greater ΔCO_2 increase at BAL (1.6 ppm yr^{-1} compared to 1.0 ppm yr^{-1}). This sensitivity test demonstrates that the increase of ΔCO_2 between 1995–2000 and 2000–2005 is robust to the flask data selection and to shifts in sampling time for BSC.

5. Can atmospheric boundary layer height explain the ΔCO_2 trend?

Now we investigate if changes in vertical dilution of surface fluxes can explain the observed increase in ΔCO_2 between 1995–2000 and 2000–2005. The contribution of transport could be further investigated using models, prescribed for instance with climatological/variable fluxes. An example of such modelling study is provided in a companion paper (Aulagnier et al., 2009). Here, we try to diagnose changes in vertical transport by using a simple variable, the height of the boundary layer, h. The value of h directly controls the vertical dilution of fluxes. In daytime, h defines the top of the well-mixed convective boundary layer, and changes in h are expected to scale linearly with changes in boundary layer mean CO_2 concentration, if the surface fluxes are constant otherwise. Obviously, in addition to pure dilution, changes in horizontal advection and in mixing by entrainment of tropospheric air into the boundary layer will also contribute to ΔCO_2 changes, but these processes are ignored here (see Aulagnier et al. (2009) for details).

We extracted 3-hourly h from the ECMWF short-range forecast archive. h has been diagnosed with the parcel lifting method (Troen and Mahrt, 1986). In practice, the post-processing is based on a threshold applied to the vertical profile of the bulk Richardson number (www.ecmwf.int/research/ifsdocs/CY28r1/Physics/Physics-04–09.html#wp972354, access 30 June 2008). Over each gridpoint, daily values of h simulated by the ECMWF weather forecast system are averaged each season under all weather conditions between 2001 and 2006. A linear regression of the seasonal mean value of h versus year was performed. Fig. 6 provides a map of the linear regression slope dh/dt for summer (June–August, JJA) and for winter (December–February, DJF). In JJA, there is a positive trend of increasing h across a Southwest to Northeast 'banana' spanning from the Iberian peninsula to western Poland. Maximum summer dh/dt values of 160 m yr^{-1} are found during the afternoon, but there is no discernible trend of h during the night. In DJF, there is a region with positive dh/dt values over the western Mediterranean basin, but the dh/dt slopes are smaller than in JJA (Fig. 6). There is also a small negative winter trend of h over Northwestern Europe. Over the ocean, h has no significant trend. The fact that h does not show any stepwise discontinuity in the ECMWF model during the period 2001–2006 indicates that the slope dh/dt can be safely interpreted as a physical signal, despite changes in assimilation data and in Numerical Weather Prediction model versions.

We make the null hypothesis that fossil fuel CO_2 emissions and all other transport processes except boundary layer height remained constant over 2001–2006. Then, the trend of ΔCO_2 must be proportional to the trend of h. To check on this, we

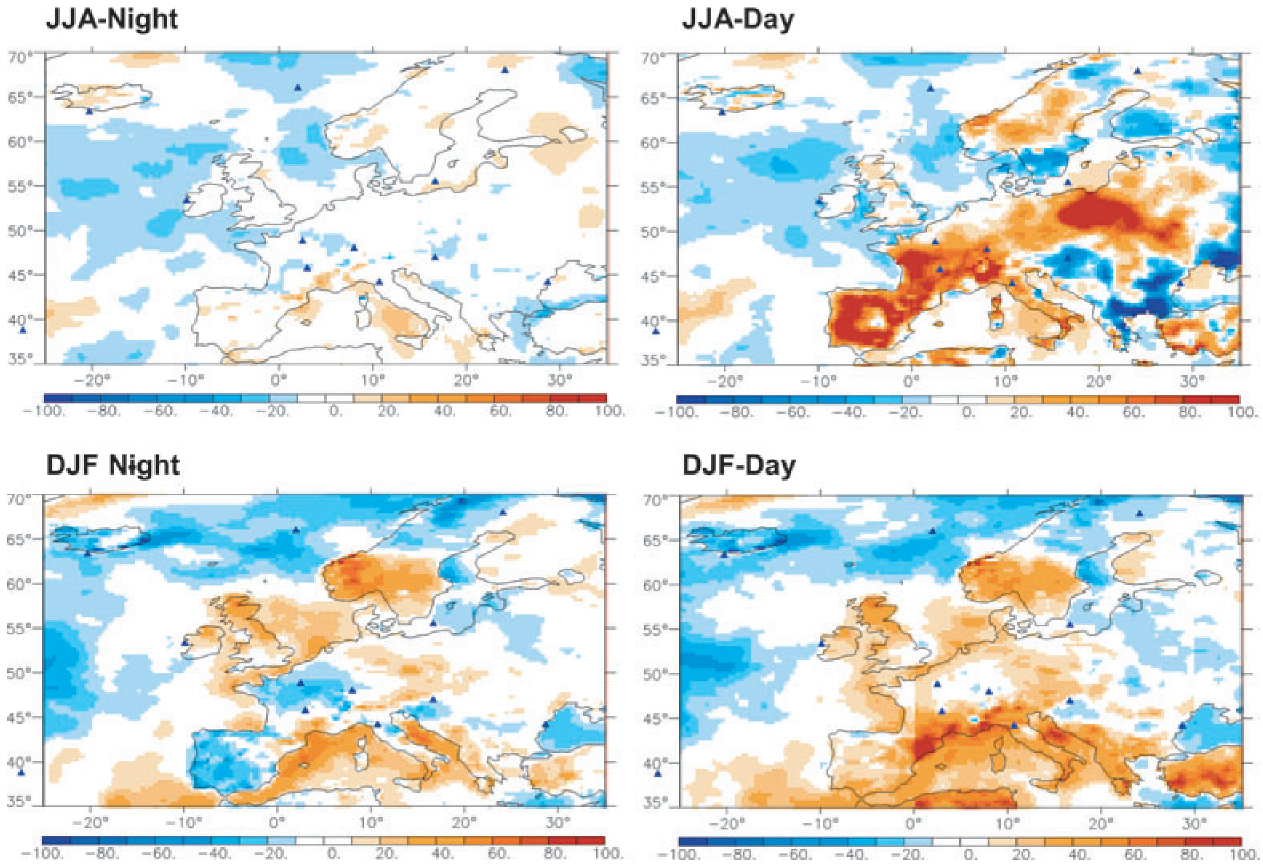

Fig. 6. Trend of the boundary layer height (m) over Europe estimated from ECMWF analyses during summer (above) and winter (below) for the period 2001–2006. The trend is calculated for afternoon (14:18 h; right) and nighttime (00:06 h; left).

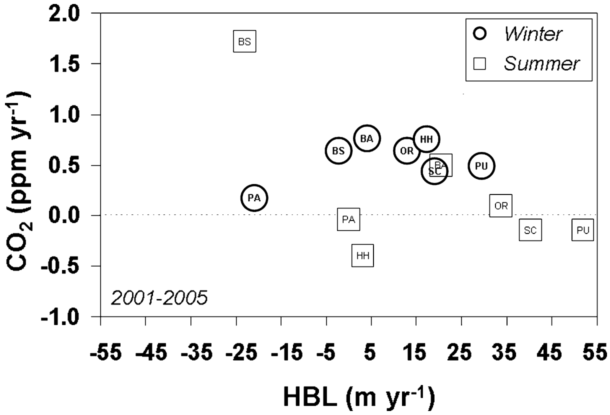

Fig. 7. Linear regression of the trend in ΔCO_2 versus the observed trend in boundary layer height h (500 km around each station). If the trend of ΔCO_2 is perfectly correlated among sites with the trend of h, then changes of h are likely to be a driver of the CO_2 build up over Europe during 2001–2005.

calculated dh/dt in a radius of 500 km around each continental station, and regressed dΔCO_2/dt as a function of dh/dt at each station for DJF and JJA, respectively. Figure 7 compares the corresponding linear regression slopes among the stations. It is observed that the trend of ΔCO_2 at each station dΔCO_2/dt is positively correlated with dh/dt, except when dh/dt reaches above 10 m yr^{-1}, where other factors may intervene to explain ΔCO_2 trends (changes in winds, or in regional fluxes). The value of R^2 suggests that 32% of the spatial variance in the trend of wintertime ΔCO_2 between stations can be explained by trends in h. In summer, there is no clear correlation between h trends and ΔCO_2 trends. Obviously, this significant positive correlation between ΔCO_2 changes and h changes illustrates the fact that h is a sensitive parameter, but a more quantitative analysis is needed. In Part 2 of this paper Aulagnier et al. (2009) apply a mesoscale transport model to these issues, and conclude similarly that boundary layers becoming more shallow can explain a significant part of the recent CO_2 build-up.

6. Trends in fossil fuel emissions impacting ΔCO_2

An alternative explanation for the observed ΔCO_2 trends is an increase of fossil CO_2 emissions in the influence of each station. The EU-25 mean fossil CO_2 emissions show only a small increasing trend of 0.5% yr^{-1} over 2001–2006, and a declining trend of -0.1% yr^{-1} over 1992–1999 (Marland et al.,

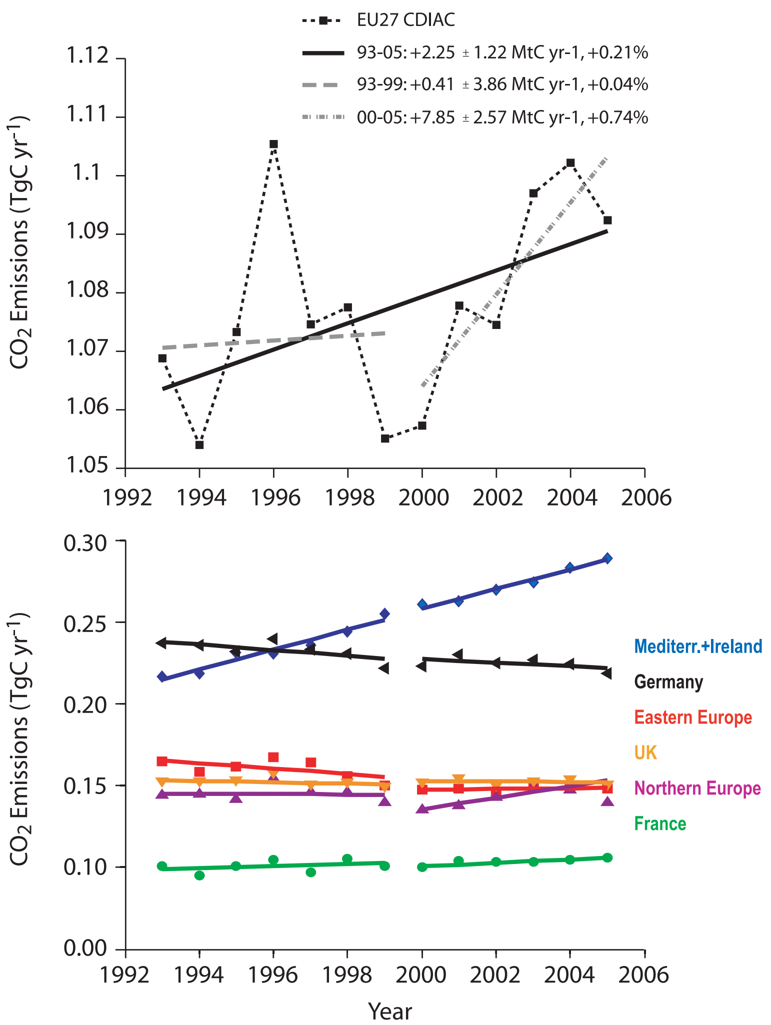

Fig. 8. Time series of fossil fuel emissions (TgC yr^{-1}) for EU27 (above) and different countries in Europe (below; Marland et al., 2007).

2007). However, this emission stability masks regionally contrasted trends. Figure 8 provides fossil fuel CO_2 emissions for six countries or groups of countries, grouped according to their similarities in emission trends: Northern Europe (Belgium, Luxembourg, Netherlands, Finland, Sweden, Denmark and Austria), Mediterranean countries (Italy, Greece, Spain and Portugal) plus Ireland, new Eastern European EU-27 member states since 2004 (Czech Republic, Estonia, Hungary, Lithuania, Latvia, Poland, Slovakia, Slovenia, Cyprus and Malta), Germany, France and UK.

In the group of Northern Europe, emissions remained stable during the 1990s, but strongly increased thereafter; by 3.8% yr^{-1}. In the Mediterranean countries grouped with Ireland, there was a fast economic growth in the past decade. For instance, the GDP annual growth was above 4% yr^{-1} in Ireland, Greece, and Spain, respectively (http://epp.eurostat.ec.europa.eu, accessed 13 June 2007). Fossil CO_2 emissions of these countries increased strongly at a rate of 2.2% yr^{-1}. This resulted in an overall multiplication by a factor of 1.2 since 1992. The 10 new Eastern European member states experienced a transition to market economies at the end of the 1990s (except for Cyprus and Malta). Emissions from these countries decreased by 1.3% yr^{-1} during 1992–1999, but this trend was reversed and emissions are now slightly increasing (+0.4% yr^{-1} over 2000–2003). Although Ukraine and Belarus are not part of the EU-27, it is interesting to remark that their collective emissions declined at an even more pronounced rate (by 9.8% yr^{-1}) than in the new EU-27 Eastern European countries between 1992 and 1999, but that this trend was reversed after 2000.

Germany is the biggest European fossil fuel CO_2 emitter (Fig. 8). Its emissions declined at a rate of 0.9% yr^{-1} after the reunification with the former Eastern Germany, and then stabilized after 2000. In France, emissions are lower than in the UK and Germany, partly because of the large share of nuclear power in electricity production. But, French emissions increased by 1.5% yr^{-1} after 2000, due largely to the transport

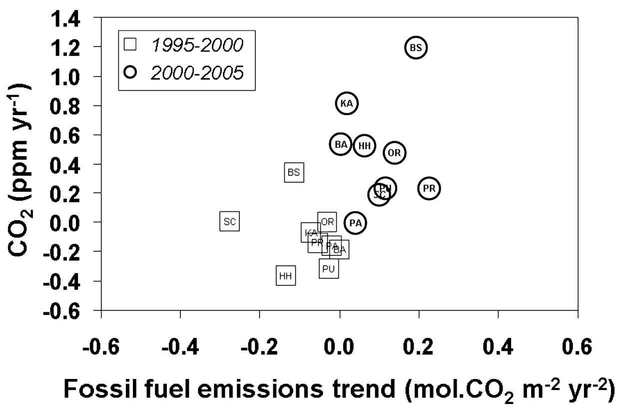

Fig. 9. Linear regression of the trend in ΔCO_2 versus the trend in fossil fuel emissions for the periods 1995–2000 and 2000–2005 (1° around each station). The fossil fuel emission trends are estimated using the mean emission value around each site from IER inventory and the national trends from CDIAC (Marland et al., 2007). An average of emission trends from France and Germany is used for Schauinsland, and emission trends from France are used for Plateau Rosa.

sector. In the UK, fossil emissions show no significant trend (0.04% yr^{-1} over the period 1992–2003), with an increase in the transportation sector offsetting a decreasing trend in emissions associated with energy production.

We make here the null hypothesis that emission trend, dF/dt, can explain the trend of ΔCO_2. Then, the $d\Delta CO_2/dt$ must be proportional to the trend of dF/dt. A rough estimate of dF/dt in a radius of 100 km of each station is calculated from each country's emission statistics. This is very coarse approximation, as it neglects seasonal, sectorial and regional emission trends, which are likely to be significant. We regressed $d\Delta CO_2/dt$ as a function of dF/dt in Fig. 9. Comparing the linear regression slope among the stations in Fig. 9, it is observed that $d\Delta CO_2/dt$ is significantly correlated with dF/dt. The value of R^2 (0.27) suggests that 27% of the spatial variance in the trend of ΔCO_2 between stations can be explained by regional trends of fossil CO_2 emissions. Obviously, more investigations of the coupling between transport changes and regionally distinct fossil CO_2 emission changes must be performed. In a first attempt to model variable NEE, fossil fuel CO_2 emissions and transport impacting ΔCO_2 changes, Aulagnier et al. (2009) using the mesoscale model CHIMERE found that transport changes (both boundary layer height and wind speed) seem to be the dominant cause of ΔCO_2 changes. However, more information on regional redistribution of emissions, with decreasing industrial emissions and increasing transportation emissions is needed, coupled with transport model simulations.

7. Conclusion

Atmospheric CO_2 is monitored over Europe for more than 10 yr at many stations, either by flask or by continuous measurements. We analysed the interannual to decadal variability of the CO_2 gradient (ΔCO_2) between continental stations and Atlantic Ocean stations which define the background air. We used the MHD station marine selected CO_2 record as a reference to calculate ΔCO_2, but the variability of ΔCO_2 is robust to the choice of another Atlantic Ocean station. The empirical data selection used at some continental stations to filter out the influence of local CO_2 sources also plays no role in the ΔCO_2 variability. We found that the interannual variability of ΔCO_2 is larger at low altitude stations (HH1, BAL) than at mountain top stations. During the extreme drought year of 2003, the summertime value of ΔCO_2 is found to be higher than usual, indicating that abnormal CO_2 losses by ecosystems, maybe coupled to abnormal transport patterns, have caused this signal.

But the most striking observation is that ΔCO_2 increased almost linearly between 1990–1995 and 2000–2005, by 1.65 ppm (PUY) to 3.6 ppm (HH1), that is, a 16% to 28% growth. This built up of CO_2 is predominantly a winter signal. In summer, no build-up is shown by the data (Table 2). Several processes can control this observed build-up. One can distinguish between processes related to variable carbon sources and sinks from processes related to variable transport. If the build-up is explained by changes in ecosystem fluxes only, a sustained loss on the order of 0.46 Pg C per year would be required during 2000–2005. We sought for two other possible mechanisms: boundary layers height becoming more shallow over the continent, and regional re-distribution of fossil fuel CO_2 emissions causing an increased footprint of emissions at the stations. A positive correlation is found between boundary layer height changes and ΔCO_2 changes between sites. Boundary layer heights becoming more shallow can explain 32% of the build-up spatial variance. Regional changes of emissions in a radius of 500 km around each station can explain up to 27% of the variance. More insights on the effect of transport versus emission changes can be given by a transport model. Aulagnier et al. (2009) suggest that a combination of more shallow boundary layers trends and wind speed trends over 2001–2006 can reproduce the observed build-up, despite a lack of trend in fluxes. Prescribing more realistic regional trends in fossil CO_2 emissions over Europe, to account for the observed increasing transportation emissions (diffuse source) and the decreasing industrial and electricity production emissions (large point sources) still remains to be done. The uncertainty of the fossil fuel emission inventories remains a limiting factor for the analysis of the regional CO_2 trends. This uncertainty is estimated to 7% at the scale of Europe but increases for smaller scales.

The existence of decadal-scale changes in atmospheric CO_2 gradients have important implications when inverting flux trends. We recommend that similar trend analysis is applied to other long-lived tracers for which long records exist (CH_4, SF_6) to better separate transport and flux effects. We also recommend that similar analysis is expanded to ΔCO_2 decadal variability for North America and Siberia.

8. Acknowledgments

This work has been done within the framework of the EU project CARBOEUROPE-IP. The authors acknowledge the OPGC/LaMP technical staff for the operations at Puy de Dôme, to Gerry Spain for the maintenance of the CO_2 analyser at Mace Head, and more generally to all the people working at the monitoring stations to provide the long term high precision measurements. Many thanks to Anton Beljaars for his advice on the ECMWF data.

References

Aalto, T., Hatakka, J., Paatero, J., Tuovinen, J.-P., Aurela, M. and co-authors. 2002. Tropospheric carbon dioxide concentrations at a northern boreal site in Finland: basic variations and source areas. *Tellus* **54B**, 110–126.

Apadula, F., Gotti, A., Pigini, A., Longhetto, A., Rocchetti, F. and co-authors. 2003. Localization of source and sink regions of carbon dioxide through the method of the synoptic air trajectory statistics. *Atmos. Environ.* **37**, 3757–3770.

Aulagnier, C., Rayner, P., Ciais, P., Ramonet, M., Rivier, L. and co-authors. 2009. Is the recent build-up of atmospheric CO_2 over Europe reproduced by models. Part 2: an overview with the atmospheric mesoscale transport model CHIMERE. *Tellus* **61B**, doi:10.1111/j.1600–0889.2009.00443.x.

Baker, D. F., Law, R. M., Gurney, K. R., Rayner, P., Peylin, P. and co-authors. 2006. TransCom 3 inversion intercomparison: impact of transport model errors on the interannual variability of regional CO_2 fluxes, 1988–2003. *Global Biogeochem. Cycles* **20**, doi:10.1029/2004GB002439.

Biraud, S., Ciais, P., Ramonet, M., Simmonds, P., Kazan, V. and co-authors. 2000. European greenhouse gas emissions estimated from continuous atmospheric measurements and radon 222 at Mace Head, Ireland. *J. Geophys. Res.-Atmos.* **105**(D1), 1351–1366.

Bousquet, P., Gaudry, A., Ciais, P., Kazan, V., Monfray, P. and co-authors. 1997. Atmospheric concentration variations recorded at Mace-Head, Ireland, from 1992 to 1994. *Phys. Chem. Earth* **21**, 477–481.

Bousquet, P., Peylin, P., Ciais, P., Le Quéré, C., Friedlingstein, P. and co-authors. 2000. Regional changes in carbon dioxide fluxes of land and oceans since 1980. *Science* **290**, 1342–1346.

Brunke, E. G., Labuschagne, C., Parker, B., Scheel, H. E. and Whittlestone, S. 2004. Baseline air mass selection at Cape Point, South Africa: application of Rn-222 and other filter criteria to CO_2. *Atmos. Environ.* **38**, 5693–5702.

Chen, B. Z., Chen, J. M. and Worthy, D. E. J. 2005. Interannual variability in the atmospheric CO_2 rectification over a boreal forest region. *J. Geophys. Res.-Atmos.* **110**(D16), doi:10.1029/2004JD005546.

Ciais, P., Reichstein, M., Viovy, N., Granier, A., Ogee, J. and co-authors. 2005. Europe-wide reduction in primary productivity caused by the heat and drought in 2003. *Nature* **437**, 529–533.

Conway, T. J., Tans, P. P. and Waterman, L. S. 1994. Atmospheric CO_2 records from sites in the NOAA/CMDL air sampling network. In: *Trends '93: A Compendium of Data on Global Change* (eds T. A. Boden, D. P. Kaiser, R. J. Sepanski and F. W. Stoss). ORNL/CDIAC-65, Oak Ridge, Tenn., USA, 41–119.

Eneroth, K., Aalto, T., Hatakka, J., Holmen, K., Laurila, T. and co-authors. 2005. Atmospheric transport of carbon dioxide to a baseline monitoring station in northern Finland. *Tellus* **57B**, 366–374.

Fink, A., Brücher, T., Krüger, A., Leckebusch, G. C., Pinto, J. G. and co-authors. 2004. The 2003 European summer heatwaves and drought—synoptic diagnosis and impacts. *Weather* **59**, 209–216.

Gerbig, C., Lin, J. C., Munger, J. W. and Wofsy, S. C. 2006. What can tracer observations in the continental boundary layer tell us about surface-atmosphere fluxes? *Atmos. Chem. Phys.* **6**, 539–554.

GLOBALVIEW-CO_2. 2006. *Cooperative Atmospheric Data Integration Project–Carbon Dioxide*. NOAA/CMDL, Boulder, CO.

Gurney, K. R., Law, R., Denning, S., Rayner, P., Baker, D. and co-authors. 2002. Towards robust regional estimates of CO_2 sources and sinks using atmospheric transport models. *Nature* **415**, 626–630.

Haszpra, L., 1999. On the representativeness of carbon dioxide measurements. *J. Geophys. Res.-Atmos.* **104**(D21), 26 953–26 960.

Haszpra, L., Barcza, Z., Bakwin, P. S., Berger, B. W., Davis, K. J. and co-authors. 2001. Measuring system for the long-term monitoring of biosphere/atmosphere exchange of carbon dioxide. *J. Geophys. Res.-Atmos.* **106**(D3), 3057–3069.

Janssens, I. A., Freibauer, A., Ciais, P., Smith, P., Nabuurs, G. J. and co-authors. 2003. Europe's terrestrial biosphere absorbs 7 to 12% of European anthropogenic CO_2 emissions. *Science* **300**, 1538–1542.

Levin, I., Glatzel-Mattheier, H., Marik, T., Cuntz, M., Schmidt, M. and co-authors. 1999. Verification of German Methane emissions inventories and their recent changes based on atmospheric observations. *J. Geophys. Res.-Atmos.* **104**(D3), 3447–3456.

Levin, I., Graul, R. and Trivett, N. B. A. 1995. Long term observations of atmospheric CO_2 and carbon isotopes at continental sites in Germany. *Tellus* **47B**, 23–34.

Marland, G., Boden, T. A. and Andres, R. J. 2007. Global, regional, and national CO_2 emissions, In: *Trends: A Compendium of Data on Global Change*. (ed. U.S. Department of Energy, Oak Ridge). Ridge National Laboratory, Carbon Dioxide Information Analysis Center, Oak Ridge, Tenn., U.S.A., doi:10.3334/CDIAC/00001.

Nabuurs, G. J., Pussinen, A., Karjalainen, T., Erhard, M. and Kramer, K. 2002. Stemwood volume increment changes in European forests due to climate change—a simulation study with the EFISCEN model. *Global Change Biology* **8**, 304–316.

Navascues, B. and Rus, C. 1991. Carbon dioxide observations at Izaña baseline station, Tenerife (Canary Islands): 1984–1988. *Tellus* **43B**, 118–125.

Necki, J., Schmidt, M., Rozanski, K., Zimnoch, M., Korus, A. and co-authors. 2003. Six-year record of atmospheric carbon dioxide and methane at a high-altitude mountain site in Poland. *Tellus* **55B**, 94–104.

Nicholls, M. E., Denning, A. S., Prihodko, L., Vidale, P. L., Baker, I. and co-authors. 2004. A multiple-scale simulation of variations in atmospheric carbon dioxide using a coupled biosphere-atmospheric model. *J. Geophys. Res.-Atmos.* **109**(D18), doi:10.1029/2003JD004482.

Pearman, G. I. 1993. Survey of results of the 1991–1992 round-robin inter-laboratory intercomparison. WMO/GAW.

Perez-Landa, G., Ciais, P., Sanz, M. J., Gioli, B., Miglietta, F. and co-authors. 2007. Mesoscale circulations over complex terrain in the Valencia coastal region, Spain. Part 1: simulation of diurnal circulation regimes. *Atmos. Chem. Phys.* **7**, 1835–1849.

Peylin, P., Bousquet, P., Le Quéré, C., Sitch, S., Friedlingstein, P. and co-authors. 2005. Multiple constraints on regional CO_2 flux variations over land and oceans. *Global Biogeochem. Cycles* **19**, doi:10.1029/2003GB002214.

Ramonet, M. and Monfray, P. 1996. CO_2 Baseline concept in 3-D atmospheric transport models. *Tellus* **48B**, 502–520.

Reichstein, M., Subke, J. A., Angeli, A. C. and Tenhunen, J. D. 2005. Does the temperature sensitivity of decomposition of soil organic matter depend upon water content, soil horizon, or incubation time? *Global Change Biol,* **11**, 1754–1767.

Rödenbeck, C., Houweling, S., Gloor, M. and Heimann, M. 2003. CO_2 flux history 1982–2001 inferred from atmospheric data using a global inversion of atmospheric transport. *Atmos. Chem. Phys.* **3**, 1919–1964.

Schmidt, M., Graul, R., Sartorius, H. and Levin, I. 1996. Carbon dioxide and methane in continental Europe: a climatology, and ^{222}Radon-based emission estimates. *Tellus* **48B**, 457–473.

Schmidt, M., Graul, R., Sartorius, H. and Levin, I. 2003. The Schauinsland CO_2 record: 30 years of continental observations and their implications for the variability of the European CO_2 budget. *J. Geophys. Res.-Atmos.* **108**(D19), doi:10.1029/2002JD003085.

Sellegri, K., Laj, P., Peron, F., Dupuy, R., Legrand, M. and co-authors. 2003. Mass balance of free tropospheric aerosol at the Puy de D(o)over-capme (France) in winter. *J. Geophys. Res.-Atmos.* **108**(D11), doi:10.1029/2002JD002747.

Szopa, S., Hauglustaine, D. A. and Ciais, P. 2007. Relative contributions of biomass burning emissions and atmospheric transport to carbon monoxide interannual variability. *Geophys. Res. Lett.* **34**(18), doi:10.1029/2007GL030231.

Thoning, K. W., Tans, P. P. and Komhyr, W. D. 1989. Atmospheric carbon dioxide at Mauna Loa Observatory, 2: analysis of the NOAA GMCC data, 1974, 1985. *J. Geophys. Res.* **94**(D6), 8549–8565.

Troen, I. and Mahrt, L. 1986. A simple model of the atmospheric boundary layer: sensitivity to surface evaporation. *Bound.-Layer Meteorol.* **37**, 129–148.

UNFCCC 2006. National greenhouse gas inventory data for the period 1990–2004 and status of reporting. UNFCCC, Framework Convention on Climate Change, Nairobi.

Vautard, R., Honore, C., Beekmann, M. and Rouil, L. 2005. Simulation of ozone during the August 2003 heat wave and emission control scenarios. *Atmos. Environ.* **39**, 2957–2967.

Vetter, M., Churkina, G., Jung, M., Reichstein, M., Zaehle, S. and co-authors. 2007. Analyzing the causes and spatial pattern of the European 2003 carbon flux anomaly in Europe using seven models. *Biogeosci. Discuss.* **4**, 1201–1240.

Yi, C., Davis, K. J., Bakwin, P. S., Denning, A. S., Zhang, N. and co-authors. 2004. Observed covariance between ecosystem carbon exchange and atmospheric boundary layer dynamics at a site in northern Wisconsin. *J. Geophys. Res.-Atmos.* **109**(D8), doi:10.1029/2003JD004164.

Supporting Information

Additional Supporting Information may be found in the online version of this article:

Text. Description of the monitoring sites.
Figure S1. Seasonal trends.
Figure S2. Sensitivity to the marine reference.
Figure S3. Sensitivity to the data selection.
Figure S4. Sensitivity to flask sampling time.

Please note: Wiley-Blackwell are not responsible for the content or functionality of any supporting materials supplied by the authors. Any queries (other than missing material) should be directed to the corresponding author for the article.